Effect of nitrogen passivation on interface composition and physical stress in SiO_2/SiC(4H) structures

Xiuyan Li,[1,2,3,a)] Sang Soo Lee,[4] Mengjun Li,[2] Alexei Ermakov,[2] Jonnathan Medina-Ramos,[4] Timothy T. Fister,[4] Voshadhi Amarasinghe,[2] Torgny Gustafsson,[3] Eric Garfunkel,[2] Paul Fenter,[4] and Leonard C. Feldman[3,5]

[1]*National Key Laboratory of Science and Technology on Micro/Nano Fabrication, Department of Micro/Nano Electronics, School of Electronic Information and Electrical Engineering, Shanghai Jiao Tong University, Shanghai 200240, People's Republic of China*
[2]*Department of Chemistry and Chemical Biology, Rutgers University, Piscataway, New Jersey 08854, USA*
[3]*Department of Physics and Astronomy, Rutgers University, Piscataway, New Jersey 08854, USA*
[4]*Chemical Science and Engineering Division, Argonne National Laboratory, Lemont, Illinois 60439, USA*
[5]*Department of Materials Science and Engineering, Rutgers University, Piscataway, New Jersey 08854, USA*

(Received 11 July 2018; accepted 10 September 2018; published online 24 September 2018)

The electron density and physical stress at the thermally oxidized SiC/SiO_2 interface, and their change with nitrogen incorporation, were observed using x-ray reflectivity, Raman scattering, and *in-situ* stress measurement. There is no evidence for residual carbon species at the SiO_2/SiC. Instead, a ~1 nm thick low electron density layer is formed at this interface, consistent with interfacial suboxides (SiO_x, $0.3 < x < 2$), along with high interfacial stress. Nitrogen passivation, a known process to improve the interface state density and electronic properties, eliminates the low density component and simultaneously releases the interface stress. On the basis of these findings, a chemical interaction model is proposed to explain the effect of the nitrogen in terms of both stress reduction and elemental control of the dielectric/SiC interface, resulting in a higher quality gate stack on SiC. *Published by AIP Publishing*. https://doi.org/10.1063/1.5048220

The 4H poly-type of silicon carbide (SiC) is being intensively studied as a suitable semiconductor for metal-oxide-semiconductor (MOS)-type power devices due to its wide bandgap, high breakdown electric field strength, and high thermal conductivity.[1,2] It is well-known that the thermally grown SiO_2 dielectric on SiC is chemically similar to that of an SiO_2 oxide grown on Si, an important technological advantage.[3] However, the relatively poor semiconductor/dielectric interface limits the mobility and reliability of SiC metal-oxide-semiconductor field-effect-transistors (MOSFETs).[4,5] A nitric oxide post-oxidation annealing (NO-POA) process helps to passivate the defects significantly by incorporating N at the interface.[6–8] This improvement has enabled the commercialization of SiC MOSFETs. Nevertheless, the device performance is still far from that anticipated by scaling similar devices such as standard Si MOSFETs. Therefore, a comprehensive understanding of the microscopic properties of as-grown and N-passivated SiO_2/SiC interfaces, namely, understanding of the physical origin of SiO_2/SiC interface states and its passivation by N, is central to the further development of SiC power devices.

An atomistic description of amorphous-single crystal interfaces is a continuing challenge in modern materials science, in part at least due to the challenge of probing buried interfaces. Early work suggested that the source of interface defects was the result of residual carbon left at the oxide/semiconductor interface.[9,10] Up to now, there is no definitive evidence of such a carbon accumulation although detection can be difficult at the low concentrations of interest. A recent high-resolution electron energy loss spectroscopy (EELS) study showed a transition layer between SiC and SiO_2 and its reduction by N incorporation[11] although the composition and structure of the transition layer was not determined. In addition, calculations suggest that the stress induced in SiC oxidation may result in interface defects like Si-Si covalent bonds (also referred to as a silicon suboxide (SiO_x) or E center),[12] but there is still no experimental confirmation. Thus, two key questions remain: (i) what is the structure, composition, and physical origin of the interface region between SiO_2 and SiC? (ii) How do N and the NO-POA modify the interface structure? In this paper, we report the systematic studies of these issues using x-ray reflectivity (XRR) supported by other interfacial probes, aimed toward a deeper understanding of these critical heterostructures.

XRR is a powerful probe of microscopic structure of buried interfaces.[13] XRR directly probes electron density profiles across buried interfaces and is well-suited to probe the SiO_2/SiC interface where the density difference is ~40%. Our XRR results, together with a combination of stress measurements, provide deep insights into the long-standing issue of the correlation between atomic-scale chemistry, physical stress, and, by inference, the interface electrical properties.

Substrates, n-type 4° off-axis 4H-SiC(0001) with a doping concentration of $\sim 10^{18}\,cm^3$, were obtained from II-VI Incorporated. The substrates were cleaned by the RCA process, followed by thermal oxidation at 1150 °C under 1 atm flowing O_2. Films of 5–50 nm SiO_2 thickness, determined by ellipsometry, were grown via control of the oxidation time varying from 40 min–20 h. For some samples, a post-oxidation-anneal was carried out at 1175 °C in 1 atm NO or Ar

a)Author to whom correspondence should be addressed: xyli06052011@gmail.com. Telephone: +1-848-445-8226.

gas. High-resolution XRR was employed to determine the electron density profile from the SiO_2 surface to the SiC substrate. The experiments were conducted at the Advanced Photon Source in Argonne National Laboratory. The monochromatic X-ray photon energy was 20 keV ($\lambda = 0.62$ Å). The specular XRR signal was measured as a function of vertical momentum transfer Q. Low-angle X-ray reflectivity data were analyzed with the MotoFit software package using a density profile consisting of slabs that were characterized by electron densities and thicknesses of the layers, and interfacial roughness between the layers.[14] The depth resolution was ~3 Å.[15] In a separate study, *in-situ* stress apparatus, capable of measuring stress at the actual oxidation temperatures, was employed to determine the chemistry-induced intrinsic stress in the SiO_2 film of SiO_2/SiC interface during SiC oxidation and NO-POA. The details of the measurement are described elsewhere.[16] In addition, Raman spectroscopy equipped with a $\lambda = 325$ nm HeCd laser was used to investigate the microscopic stress on as-grown and NO-annealed SiC samples. A mapping of measurements over 128 different points over a 8×8 μm^2 section was averaged to get a statistically relevant result.

As suggested by x-ray photoelectron spectroscopy (XPS) and other results, we anticipate that the interface contains a non-stoichiometric dielectric layer.[17,18] However, with probes like XPS and EELS, it is difficult to identify the non-stoichiometric material among various candidates, such as sub-oxides of SiO_2 and/or SiC_xO_y composites, because both show similar Si binding energies with intermediate oxidation, while a small amount of carbon signal is indistinguishable from surface adsorbates. Here, we calculate the electron density of various possible species in the SiO_2/SiC interface relative to that of SiC and SiO_2, as summarized in Table I. The calculation method is described in the supplementary material (Fig. SI). The compound SiO_x with $0.3 < x < 2$ has a lower electron density than SiO_2, while carbon containing species such as SiO_xC_y or graphite have a higher density. XRR can determine the electron density of an individual layer with a high precision, e.g., typically within <1% error (see Fig. SII and Table SI in the supplementary material for details), thereby allowing us to distinguish small differences in the layer density at the interface. This means that XRR can distinguish a SiO_x type of interfacial material from a carbon related species. In addition, XRR also enables a distinction between various features of the derived interfacial structure (including the density and thickness of interfacial layers) and the roughness as described in Fig. SII and Table SI.

A schematic of the XRR experiment is shown in Fig. 1 along with results for as-grown SiO_2/SiC stacks and the best fit model. We note the very high quality of the fit to the reflectivity data using a three layer model [Fig. 1(c)] with a

TABLE I. The electron density for materials of interest at the SiO_2/SiC and SiO_2/N/SiC interfaces.

Parameters	SiO_2	SiC	Graphite	$SiO_{x(0.3<x<2)}$	SiO_xC_y	Si_3N_4
Electron density ($e^-/Å^3$)	0.662	0.964	0.683	0. 640–0.662	0.662–0.964	0.95
$\rho_e/\rho_{e\text{-}(SiC)}$	0.686	1	0.708	0.66–0.686	0.686–1	0.99

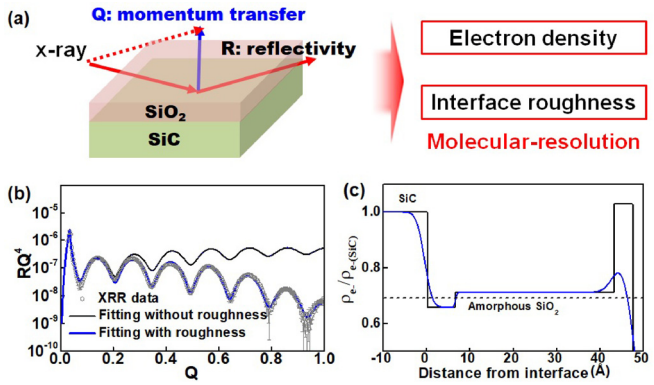

FIG. 1. (a) Schematic of XRR measurement of SiO_2/SiC structures. (b) The Fresnel normalized XRR data [i.e., $R(Q) \times Q^4$] of a SiO_2(5 nm)/SiC sample with simulated results of a three-layer-model, both with and without considering roughness. (c) Electron density depth profiles from the SiO_2 surface through the SiC substrate obtained from the simulated models in (b).

structure that reproduces the expected density of an amorphous SiO_2 film at some distance from the interface. (Parameters and uncertainties of best model are summarized in Table SI, and poorer fits that occur with one and two layer models are shown in Fig. SII.) Interestingly, an anomalous interface feature at the SiO_2/SiC interface is observed with a ~0.5 nm thickness (half-width at half minimum) and an electron density that is ~6% *lower* than SiO_2. Based on Table I, this layer is interpreted as a SiO_x suboxide ($0.3 < x < 2$). This means that the non-stoichiometric interface between SiO_2 and SiC is associated with SiO_x rather than SiO_xC_y or other higher density carbon-containing phases. This is consistent with our previous medium energy ion spectroscopy (MEIS) results showing no excess carbon at this interface within the MEIS detection limit ($\sim 5 \times 10^{14}/cm^2$).[19] Another possible explanation of a lower density interface feature is porous SiO_2. However positron annihilation experiments, which are very sensitive to interface porosity, show no evidence for such a feature.[20] The high density layer at the SiO_2 surface in Fig. 1(c) is attributed to surface contamination in the air exposure.

We have reported the areal concentration of nitrogen incorporated at the SiO_2/SiC interface resulting from varying NO-POA treatments.[21] A variety of measurements show that N accumulates at the SiC (0001)/SiO_2 interface in submonolayer amounts with a saturation value of $\sim 5 \times 10^{14}/cm^2$, roughly equivalent to half a monolayer of the atom density in 4H SiC.[19] XPS analysis by Xu *et al.*[22] indicates that the nitrogen is bonded in the form of N-Si_3. Critically, the effective inversion layer mobility of the SiC MOSFET is correspondingly enhanced by N incorporation [Fig. 2(a)].[23] We have systematically determined the interface structures of these samples by XRR [Fig. 2(b)]. Surprisingly, the low electron density layers at the as-grown SiO_2/SiC interfaces are reduced by the NO-POA process. With longer annealing times, there is a greater reduction of the low density layer consistent with more N incorporated at the interface. When N incorporation reaches saturation (>1 h), the low density layer is largely eliminated. These results clearly correlate with the mobility enhancement in Fig. 2(a).

We next consider both why the low density layer is formed and how it is modified by N incorporation. In the simplest picture, one monolayer of Si should be in an

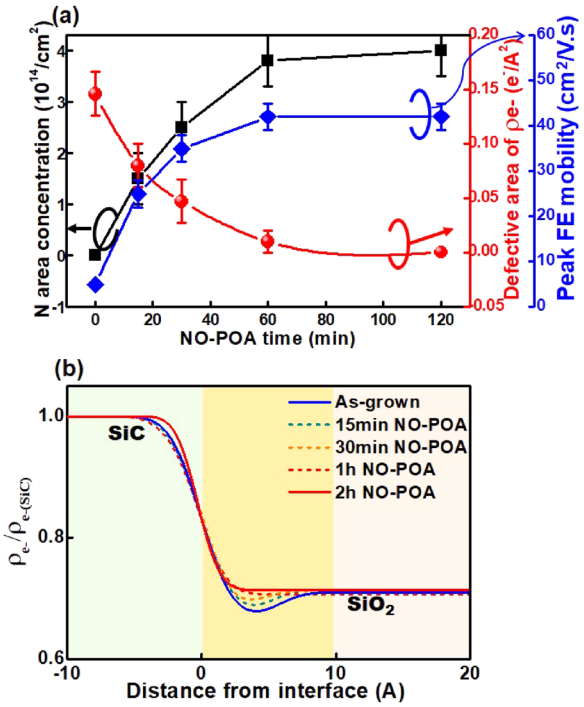

FIG. 2. (a) Area concentration of N incorporated at the SiO_2/SiC interface, area of electron density deficiency of the interfacial layer between SiO_2 and SiC [in (b)] and peak mobility of SiC MOSFET as a function of NO-POA time. (b) Depth profile of electron density from the SiO_2 surface to the SiC substrate of samples as-grown and with NO-POA for 15 min–2 h.

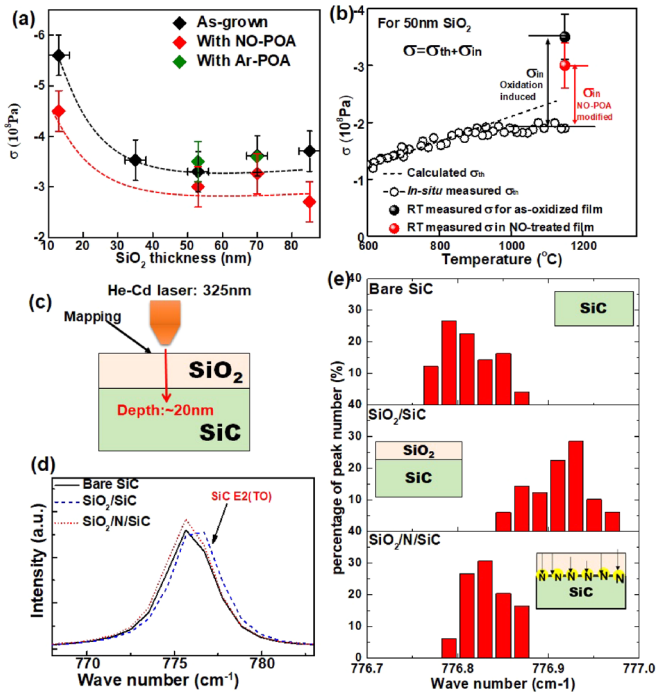

FIG. 3. (a) Total stress (σ) in SiO_2 in SiO_2/SiC structures as-grown, after Ar-POA and after NO-POA, as a function of film thickness measured at room temperature (RT). (b) Estimation of oxidation induced and NO-POA-modified intrinsic stress (σ_{in}) in 50 nm SiO_2, by subtracting thermal stress (σ_{th}) from σ. (c) Raman spectroscopy setup to measure stress at SiC surfaces. (d) SiC E_2(TO) peak evolution and (e) peak position in bare SiC-substrate, as-grown and as NO-treated SiO_2 (5–50 nm)/SiC samples.

intermediate oxidation state when SiC is bonded to bulk SiO_2, just as for Si. However, a transition region of more than a monolayer of interfacial SiO_x has been shown to exist in the SiO_2/Si system.[24,25] It has been argued that SiO_x near the interface may arise to help reduce interfacial stress caused by the 120% mismatch of Si density between SiO_2 and Si.[25,26] Coincidentally, there is also a ~120% Si density mismatch between SiC and SiO_2, consistent with more than one monolayer of SiO_x as shown above. These similarities between the Si/SiO_2 and SiC/SiO_2 systems guide us to consider interface stress as the driving force of SiO_x formation and reduction.

In order to understand the correlation between physical stress and chemical structure, we investigated the interface stress experimentally. Earlier we reported a compressive stress of $\sim 10^8$ Pa in SiO_2 films in as-grown SiO_2/SiC.[16] The Si density mismatch between the SiC substrate and the oxide induces an intrinsic stress. Here, we extract this intrinsic stress at as-grown and NO-treated SiO_2/SiC interfaces by subtracting the thermal stress (caused by thermal expansion mismatch during cooling and obtained from an *in-situ* measurement) from the total one (Fig. 3). As expected, the oxidation-induced compressive stress is partially relaxed by the NO-POA. Note that an Ar-POA at the same temperature as the NO process does not change the stress significantly. This suggests that stress relaxation by NO-POA is a compositional effect due to incorporation of N rather than solely the result of a thermal process.

We also investigated the stress on SiC from the SiC/SiO_2 interface using Raman spectroscopy. The penetration depth into SiC of the HeCd laser is estimated to be about 20 nm as schematically shown in Fig. 3(c). Thus, information from the SiC surface can be obtained. The main peak at 777 cm^{-1} in Fig. 3(d) is due to the E_2(TO) mode of SiC. Figure 3(e) shows a histogram of the Raman peak position measured on a grid of 128 points over 8×8 μm^2, for bare SiC, after oxidation and after NO-POA treatment. We find a positive peak shift after oxidation. Based on the known correlation between stress and Raman shift in 4H-SiC,[27] this shift corresponds to a compressive stress of $\sim 10^8$ Pa, consistent with our direct determination above. As expected, after an NO-POA, the Raman peak shifts back, clearly demonstrating stress relaxation upon N incorporation.

Thus, we conclude that SiO_x formation may be associated with lowering of interface stress, resulting from the Si density mismatch between SiO_2 and SiC, and that the nitridation of SiO_2/SiC may be a result of further minimization of the interface stress.

The correlation between physical stress, structure, and composition and their effect on electrical properties of the SiC/SiO_2 interface is now discussed in light of above results. Analogous to Si oxidation, a 120% volume expansion occurs during the oxidation of SiC to SiO_2, resulting in a huge stress in principle. Due to this, it is almost impossible to form a perfect, sharp interface with simple Si-oxygen bonding as its energy will be too high. Although this huge stress is significantly released by vertical viscous flow of SiO_2 with a lateral part remaining at the SiO_2/SiC interface,[16] we suggest that a portion of this stress relaxation is in the formation of a transition layer of more than one monolayer of a Si rich oxide, similar to that reported for the SiO_2/Si system.[25,26] Such a Si rich oxide consumes more Si per oxygen, partially compensating the Si density mismatch. In fact, the stress has been cited as a driving force for bonding configurations such as the Si-Si

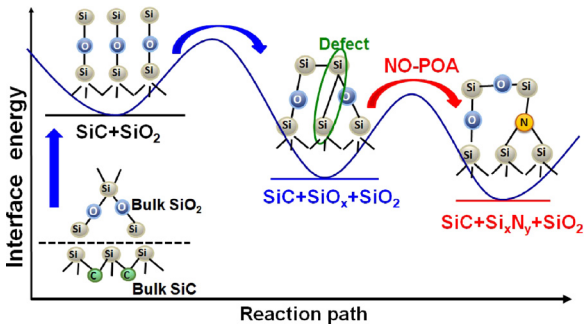

FIG. 4. (a) Energy diagram of SiO_x formation and N incorporation. Both may be attributed to lowering of strain energy caused by Si density mismatch between SiC and SiO_2. We believe that the N-Si_x interlayer is more efficient than the Si-O_x one in compensating the Si density mismatch between SiC and SiO_2.

complex, resulting in specific electrically active interfacial defects at SiO_2/SiC, in some computational work.[12]

The beneficial effect of the nitrogen addition may be understood by the following argument. Note that bulk Si atomic density in Si_3N_4 ($\sim 4 \times 10^{22}/cm^3$) is even higher than in SiO_x (such as $2.9 \times 10^{22}/cm^3$ in SiO) and close to that of SiC ($\sim 5 \times 10^{22}/cm^3$). We suggest that consumption of excess Si in SiO_x by the formation of Si_3N_4 will further reduce the interface stress and hence the interface energy. Such a mechanism may also reduce stress driven electrical defects at the interface. For specificity, we now represent SiO_x as SiO. Then, in this model, one half of the Si atoms in the SiO layer need to be converted to Si_3N_4, leaving the remainder in the form of SiO_2. To completely achieve this, for the "as-grown" structure reported here, requires the insertion of a nitrogen density of $\sim 6.6 \times 10^{14}$ atom/cm^2.

Figure 4 shows a schematic picture of the above model. A variety of measurements support this picture. The required nitrogen content is consistent with our experimental determination of a saturated nitrogen density incorporated at SiO_2/SiC interface ($\sim 5 \times 10^{14}$ atom/cm^2).[19,21] Formation of a N-Si_3 like bonding has been also shown by Xu *et al.*, as mentioned above.[22] This model naturally explains our observation that nitrogen creates a more ideal SiO_2/SiC interface structure, accompanied by a significant improvement in electronic properties. In addition, the mechanism also explains why the N incorporation saturates, an unexplained fact up until now: N accumulates only until all the "excess" Si is consumed.

In summary, our results provide deep insights into the long-standing issue of the atomic-scale mechanisms that result in the dramatic improvement of SiC MOSFET performance following nitrogen incorporation. We find (within our detection limits) no evidence for residual carbon at the interface. A SiO_x layer driven by oxidation-induced stress is observed and is attributed to be the defect structure associated with poor electrical properties. N incorporation consumes excess Si in SiO_x, releases the stress, and hence reduces the electrical defects. Thus, the manipulation of interface stress through elemental control may be the key for further progress towards high quality SiC MOSFETs.

See supplementary material for the method to calculate the electron density of materials of interest and for the detailed analysis to get the best fit model from XRR data.

This work was supported by II-VI Foundation and done partly with II-VI Incorporated. SSL, TTF, and PF were supported by the U.S. Department of Energy, Office of Basic Energy Sciences, Division of Chemical Sciences, Geosciences, and Biosciences (Geosciences Research Program) through Argonne National Laboratory. Argonne is a U.S. Department of Energy laboratory managed by UChicago Argonne, LLC, under Contract No. DE-AC02-06CH11357. We acknowledge the use of beamline 12-ID-D and 33-BM-C at the Advanced Photon Source at Argonne National Laboratory. We would like to thank Dr. A. Toriumi's group for the use of the Raman spectrometer and thank Mr. S. Ward, Dr. A. B. Mann, Mr. Y. Noma, and Dr. T. Nishimura for discussion of the Raman results.

[1]S. E. Saddow and A. Agarwal, *Advances in Silicon Carbide Processing and Applications* (Artech House, Norwood, 2004)
[2]F. Devynck, A. Alkauskas, P. Broqvist, and A. Pasquarello, Phys. Rev. B **83**, 195319 (2011).
[3]T. Kimoto and J. A. Cooper, *Fundamentals of Silicon Carbide Technology* (Wiley, Singapore, 2014), pp. 301–352.
[4]J. A. Cooper, Phys. Status Solidi A **162**, 305 (1997).
[5]L. A. Lipkin and J. W. Palmour, J. Electron. Mater. **25**, 909 (1996).
[6]G. Y. Chung, C. C. Tin, J. R. Williams, K. McDonald, M. Di Ventra, S. T. Pantelides, L. C. Feldman, and R. A. Weller, Appl. Phys. Lett. **76**, 1713 (2000).
[7]D. Okamoto, H. Yano, T. Hatayama, and T. Fuyuki, Appl. Phys. Lett. **96**, 203508 (2010).
[8]T. Kimoto, Jpn. J. Appl. Phys., Part 1 **54**, 040103 (2015).
[9]T. Zheleva, A. Lelis, G. Duscher, F. Liu, I. Levin, and M. Das, Appl. Phys. Lett. **93**, 022108 (2008).
[10]F. Amy, P. Soukiassian, Y.-K. Hwu, and C. Brylinski, Phys. Rev. B **65**, 165323 (2002).
[11]J. A. Taillon, J. H. Yang, C. A. Ahyi, J. Rozen, J. R. Williams, L. C. Feldman, T. S. Zheleva, A. J. Lelis, and L. G. Salamanca-Riba, J. Appl. Phys. **113**, 044517 (2013).
[12]K. Shiraishi, K. Chokawa, H. Shirakawa, K. Endo, M. Araidai, K. Kamiya, and H. Watanabe, in *Proceedings of the International Electronic Device Meeting (IEDM)* (IEEE, 2014), p. 21.3.
[13]M. Tidswell, B. M. Ocko, P. S. Pershan, S. R. Wasserman, G. M. Whitesides, and J. D. Axe, Phys. Rev. B **41**(2), 1111 (1990).
[14]A. Nelson, J. Appl. Crystallogr. **39**, 273 (2006).
[15]P. Fenter and Z. Zhang, Phys. Rev. B **72**, 081401(R) (2005).
[16]X. Li, A. Ermakov, V. Amarasinghe, E. Garfunkel, T. Gustafsson, and L. C. Feldman, Appl. Phys. Lett. **110**, 141604 (2017).
[17]C. Virojanadara and L. I. Johansson, Phys. Rev. B **71**, 195335 (2005).
[18]H. Watanabe, T. Hosoi, T. Kirino, Y. Kagei, Y. Uenishi, A. Chanthaphan, A. Yoshigoe, Y. Teraoka, and T. Shimura, Appl. Phys. Lett. **99**, 021907 (2011).
[19]X. Zhu, H. D. Lee, T. Feng, A. C. Ahyi, D. Mastrogiovanni, A. Wan, E. Garfunkel, J. R. Williams, T. Gustafsson, and L. C. Feldman, Appl. Phys. Lett. **97**, 071908 (2010).
[20]M. Maekawa, A. Kawasuso, M. Yoshikawa, and H. Itoh, Appl. Surf. Sci. **216**, 365 (2003).
[21]J. Rozen, S. Dhar, M. E. Zvanut, J. R. Williams, and L. C. Feldman, J. Appl. Phys. **105**, 124506 (2009).
[22]Y. Xu, X. Zhu, H. D. Lee, C. Xu, S. M. Shubeita, A. C. Ahyi, Y. Sharma, J. R. Williams, W. Lu, S. Ceesay, B. R. Tuttle, A. Wan, S. T. Pantelides, T. Gustafsson, E. L. Garfunkel, and L. C. Feldman, J. Appl. Phys. **115**, 033502 (2014).
[23]J. Rozen, A. C. Ahyi, X. Zhu, J. R. Williams, and L. C. Feldman, IEEE Trans. Electron **58**(11), 3808 (2011).
[24]F. J. Himpsel, F. R. McFeely, A. Taleb-Ibrahimi, and J. A. Yarmoff, Phys. Rev. B **38**, 6084 (1988).
[25]Z. H. Lu, S. P. Tay, R. Cao, and P. Pianetta, Appl. Phys. Lett. **67**, 2836 (1995).
[26]Y. Tu and J. Tersoff, Phys. Rev. Lett. **84**, 4393 (2000).
[27]S. H. Ward and A. B. Mann, in Gordon Research Conference (2016).